Author: Kröner, Eleanore Sophie Jeanine
Title: Magnetic resonance imaging of vessel wall morphology and function
Issue Date: 2015-06-24

CHAPTER 3

ULTRAHIGH-FIELD 7-T MAGNETIC RSONANCE CAROTID VESSEL WALL IMAGING: INITIAL EXPERIENCE IN COMPARISON WITH 3-T FIELD STRENGHT

E.S.J. Kröner, L.D. van Schinkel, M.J. Versluis, N.J. Brouwer, P.J. van den Boogaard, E.E. van der Wall, A. de Roos, A.G. Webb, H.J. Siebelink, H.J. Lamb

Invest Radiol 2012;47:697-704.

ABSTRACT

Purpose: Magnetic Resonance Imaging (MRI) of the vessel wall enables determination of luminal area, vessel wall thickness, and atherosclerotic plaque characteristics.
For clinical application, high spatial resolution, deriving from optimal signal-to-noise-ratio (SNR) and contrast-to-noise-ratio (CNR) is paramount. Vessel wall MRI is expected to benefit from higher magnetic field strength. Therefore, the purpose of the present study was to develop ultra-high field 7T MRI hardware and protocols for vessel wall imaging of the carotid artery and to compare quantitative parameters of vessel wall morphology and image quality between 3T and 7T MRI.

Methods: 18 volunteers (11 males, 7 females, mean age=29 ± 7 yrs) underwent MRI-examinations at 7T (using a custom built surface transmit/receive coil of 15 cm diameter) and at 3T (using a commercial phased-array coil with two flexible oval elements, each 14 x 17 cm). MRI of the left common carotid artery vessel-wall was performed at 7T with identical in-plane resolution as 3T MRI (0.46 x 0.46 mm^2) providing transverse T1- and T2-weighted images. Blinded analysis of morphologic measurements (lumen area and vessel wall area), SNR for vessel wall (SNR_{VW}), and the contrast-to-noise ratio between lumen and wall (CNR) were compared between 7T and 3T.

Results: Morphologic carotid vessel wall measurements were comparable between 7T and 3T for both T1-weighted images (lumen area; ICC: 0.81, vessel wall area; ICC: 0.84) and T2-weighted images (lumen area; ICC: 0.97, vessel wall area; ICC: 0.92). At 7T, SNR_{VW} and CNR were significantly higher as compared to 3T MRI for both T1- ($p<0.001$) and T2-weighted images ($P<0.05$), with gain factors ranging from 1.3 to 3.6.

Conclusions: Ultra-high field 7T MR carotid vessel wall imaging is feasible. 7T MRI of the common carotid artery has comparable accuracy for determining luminal area and vessel wall area and has improved SNR_{VW} and CNR as compared to 3T MRI. Therefore, ultra-high field 7T vessel wall MRI may enable more detailed assessment of plaque morphology.

INTRODUCTION

Atherosclerosis and its thrombotic complications are the major cause of morbidity and mortality in the industrialized countries (1). Early detection of atherosclerosis by a non-invasive imaging tool may permit optimized risk-stratification, prevention and early treatment initiation in patients with various degrees of atherosclerotic disease (2). Magnetic resonance imaging (MRI) has emerged as a promising imaging modality for studying atherosclerotic disease in humans in vivo (2).

For clinical application, high spatial resolution, deriving from optimal signal-to-noise-ratio (SNR) and contrast-to-noise-ratio (CNR) is paramount. A new generation of ultra-high field MR scanners operating at 7T has recently become available for clinical research (3-6). In many applications ultra-high field MRI provides higher SNR and CNR, which can be used to increase spatial resolution (3,7-9). Therefore, it is expected that MR imaging of the carotid vessel wall may potentially benefit from higher magnetic field strength.

At present only limited data are available on the feasibility of 7T carotid artery MRI (10). To our knowledge no comparative studies between 3T and 7T carotid artery imaging have been performed investigating vessel morphology measurements (lumen area and vessel wall area) and quantification of image quality (SNR and CNR).

Therefore, the purpose of the present study was to develop an ultra-high field 7T MRI protocol for vessel wall imaging of the carotid artery, and to compare quantitative parameters of vessel wall morphology and image quality between 3T and 7T MRI.

MATERIALS AND METHODS

Patient population and study protocol

Subjects

18 volunteers (11 males, 7 females, mean age=29 ± 7 yrs) were included. None of these volunteers had a previous history of cardiovascular disease. Approval from the local Medical Ethical Committee was obtained and all volunteers gave written informed consent.

General MRI protocol

Subjects underwent MRI examinations of the left carotid artery consecutively on 3T and 7T MR systems. Scanning was performed using commercial 3T and 7T scanners (Achieva, Philips, Best, The Netherlands). The MR systems were equipped with a commercial vector ECG module. The electrodes of the vector were placed on the anterior chest wall, with two electrodes (lead 1 (L1), L2) in the sternum, one electrode (L3) vertical to L1 and L2, just below the sternum. In addition one electrode (L4) was placed horizontal to L2, on the left thorax in the mid axillary line (5). All subjects were positioned head first and in the supine position in the scanner.

Similar protocols were employed at both MR field strengths: After acquisition of a three-dimensional (3D) time-of-flight (TOF) sequence to localize the vessel bifurcation, sagittal and coronal 2D survey scans of the left carotid artery were acquired. The multi-contrast carotid vessel wall protocol was planned on these images and consisted of a T1 fast gradient echo (FGE) sequence, a T2 turbo spin echo (TSE) sequence and a 3D TOF sequence. The scan parameters for the multi-contrast protocol at 3T and 7T field strength are given in the next section and an overview is provided in Table 1. The main difference between the T1-weighted protocols at 7T and 3T is that 7T black blood (BB) preparation was performed using local saturation slabs saturating the inflowing venous and arterial blood. In contrast, at 3T BB preparation was performed by a global inversion followed by a slice-selective 10 mm thick re-inversion using the body coil. The difference in BB preparation between 7T and 3T is due to the absence of a body coil at 7T MR system and limited RF coverage of the transmit/receive (T/R) coil at 7T. For the T2-weighted TSE protocols no BB prepulse was used. For the TOF images a saturastion slab superior to the imaging stack was placed at 3T, which was not the case at 7T.

Table 1. Scan parameters for Carotid Vessel Wall Imaging Protocols at 3T and 7T

	Black-blood T1-weighted	Black-blood T1-weighted	Black-blood T2-weighted	Black-blood T2-weighted	Time-of-Flight	Time-of-Flight
	3T	7T	3T	7T	3T	7T
Acquisition sequence	FGE	FGE	TSE	TSE	FFE	FFE
Acquisition mode	2D	2D	2D	2D	3D	3D
Echo time (ms)	3.5	3.7	50	50	3.30	3.6
Repetition time (ms)	12.4	13	2 heartbeats	2 heartbeats	26.20	15
Excitation flip angle (degrees)	45	45	90	90	20	20
FOV (mm)	140 x 140	140 x 140	140 x 140	140 x 140	140 x 140	140 x 140
Resolution (mm2)	0.46 x 0.46	0.46 x 0.46	0.46 x 0.46	0.46 x 0.46	0.46 x 0.46	0.46 x 0.46
Slice thickness / gap (mm)	2; 0.7	2; 0.7	2; 0.7	2; 0.7	2; 0.7	2; 0.7

Abbreviations: 3T, 3 Tesla magnetic field strength; 7T, 7 Tesla magnetic field strength; FGE, gradient echo; TSE, turbo segmented spin-echo; FOV, field of view

3T MRI acquisition

RF coil

A standard Philips SENSE-flex-M surface coil with two flexible elements of 14×17cm was positioned around the neck, as previously described (11). An example of coil positioning at 3T and 7T is provided in Figure 1.

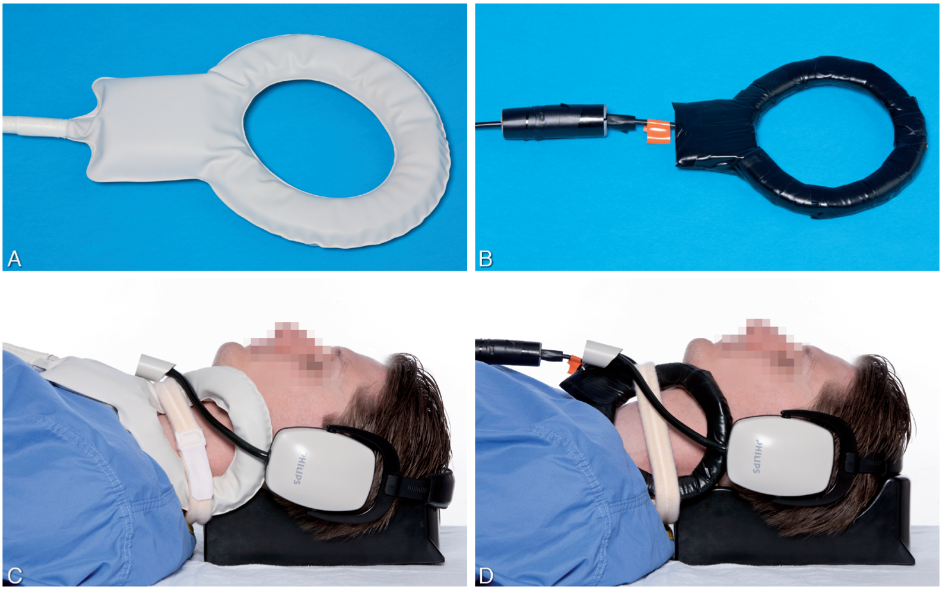

Figure 1. A: Standard Philips SENSE-flex-M surface coil (14 x 17 cm) used for the 3T MR acquisition is shown. **B:** Custom-built local surface transmit/receive coil of 15-cm diameter used for the 7T acquisition is shown. **C:** Coil positioning and scanning set-up at 3T MRI. **D:** Coil positioning and scanning set-up at 7T.

Survey

The 3T protocol has been previously described (11). In short, two survey scans in sagittal and coronal direction were planned on a 3D TOF sequence scout scan.

Multicontrast 3T protocol

Subsequently the multi-contrast 3T protocol, including three sequences were planned on the two surveys scans, perpendicular to the course of the common carotid artery in both views. Nine contiguous transverse slices of 2-mm thickness, with identical in-plane resolution (0.46×0.46mm^2), were positioned with the middle of the stack (slice number 5) at the level of the carotid bifurcation of the left carotid artery. The scan parameters were:

1: 2D BB T1-weighted fast gradient echo (FGE) sequence (scan parameters; field-of-view (FOV) 140 x 140 mm, 2.0 mm slice thickness, repetition time (TR): 12.41 ms / echo time (TE): 3.54 ms / flip angle (FA): 45º, acquired pixel size 0.46 x 0.46 x 2 mm^3, scan duration per slice = 1.3 minutes at a typical heart rate of 65 beats per minutes, ECG triggering at end-diastole), with up to second order shimming.

2: 2D BB T2-weighted turbo spin echo (TSE) sequence (scan parameters; FOV 140 x 140 mm, 2.0 mm slice thickness, TR / TE / FA: 2 heartbeats/ 50 ms / 90º, acquired pixel size 0.46 x 0.46 x 2 mm^3, scan duration per slice = 1.5 minutes at a typical heart rate of 65 beats per minutes, ECG triggering at end-diastole), using linear shimming.

All BB images were obtained with spectral presaturation inversion recovery (SPIR) fat suppression.

3: 3D TOF sequence (scan parameters; FOV: 300 x 300 mm, 2.0 mm slice thickness, TR / TE / FA: 26.20 ms / 3.3 ms/ 20º, acquired pixel size 0.46 x 0.46 x 2 mm^3, scan duration per slice = 0.4 minutes, acquired without ECG-triggering), using linear shimming.

7T MRI acquisition

RF Coil

A 15-cm diameter local surface T/R surface coil was locally developed. The coil was segmented into six sections by series connected non-magnetic capacitors (American Technical Ceramics). The coil was positioned at the left side of the neck. A cushion was used to fix the position of the neck (Figure 1).

Survey Scans

Three FGE sequence survey scans were performed to facilitate planning of the carotid vessel wall protocol. A 2D TOF sequence was acquired with the following parameters, voxel size = 1 x 1.2 x 5 mm^3 and a FOV= 300 x300 mm^2, 20 transverse slices, TR/ TE/ FA= 7.7 ms / 3.7 ms / 20°, during free breathing and without using ECG triggering. The scan covered 10 cm of the left carotid artery in 38 seconds scan duration. The second survey was planned by defining three points in the center of the common, internal and external carotid arteries, which resulted in an oblique sagittal view of the carotid bifurcation. The third survey was planned in an oblique sagittal plane. The survey scans were acquired using a single slice ECG triggered FGE following parameters: voxel size = 0.46 x 0.47 x 2.5 mm^3, FOV = 140 x 140 mm^2, TR /TE / FA = 12 ms / 3.6 ms / 20°, resulting in an average scan duration of 56 seconds each.

Multi Contrast 7T protocol

Subsequently the multi-contrast 7T protocol, including three sequences were planned on the two surveys scans, perpendicular to the course of the common carotid artery in both views. To ensure registration between 7T and 3T scans, the 7T images, consisting of five contiguous transverse slices of 2-mm thickness, with identical in-plane resolution as 3T (0.46×0.46mm^2), were positioned with the top-slice at the level of the carotid bifurcation of the left carotid artery. Acquisition of slices continued in the proximal (caudal) direction covering 1.0 cm of the left common carotid artery.

A localized tip angle calibration was performed as a preparation step before the actual sequences to calibrate the tip angle in the target region (12), and linear shimming was performed in the same region. The scan parameters were:

1: 2D BB T1-weighted FGE sequence (scan parameters: FOV = 140 x 140 mm^2, TR / TE / FA = 13 ms / 3.7 ms / 45°, scan duration per slice = 1.25 minutes at a typical heart rate of 65 beats per minutes). Three saturation slabs (35 mm thickness), consisting of pairs of manufacturer provided adiabatic RF pulses, were used (two were placed inferior, and one superior and performed interleaved) to suppress flowing blood after which 8 excitations were performed, with linear profile encoding. The slices were measured sequentially and the saturation slabs followed each slice to obtain optimal blood suppression. Acquisitions were triggered to end diastole.

2: 2D BB T2-weighted fat suppressed TSE sequence (scan parameters: FOV = 140 x140 mm^2, TR / TE / FA = 2 heartbeats / 50 ms / 90°, TSE factor = 8, scan duration per slice = 1.2 minutes at a typical heart rate of 65 beats per minutes). Cardiac triggering was performed at end diastole. Fat suppression was performed using a spectrally selective adiabatic inversion pulse to improve the homogeneity of the suppression.

3: 3D TOF sequence (scan parameters: FOV = 140 x 140 mm^2, TR / TE / FA = 15 ms / 3.6 ms / 20°, scan duration per slice = 0.3 minutes, acquired without ECG-triggering).

MR analysis

The cross-sectional images of the three sequences for the 3T and 7T scans were matched using the bifurcation of the carotid artery as a marker. The 3T and 7T analysis of morphologic measurements and measurements of image quality was performed on one slice of

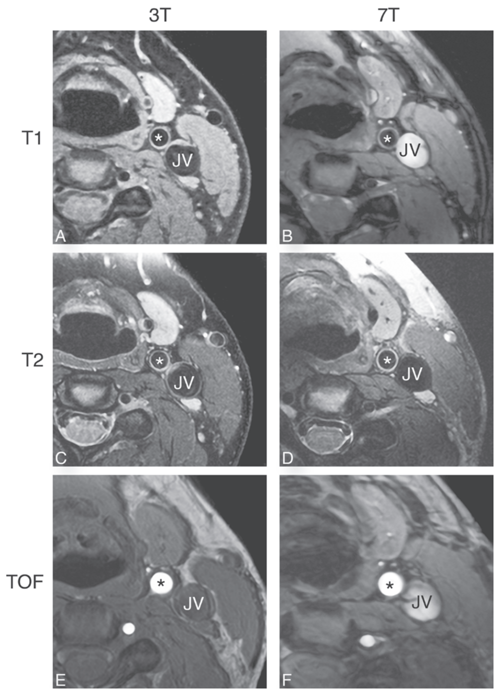

Figure 2. Example of multi-contrast black-blood images (T1- and T2-weighted) and time-of-flight image (TOF) of the left carotid artery obtained on 3T and 7T scanners with identical spatial resolution. From top to bottom: scout, T1-weighted fast gradient echo (T1), T2-weighted turbo spin echo (T2) and time-of-flight (TOF). Asterisks are provided on the transverse slices to indicate vessel lumen.

Abbreviations: 3T, 3 Tesla magnetic field strength; 7T, 7 Tesla magnetic field strength; T1, T1-weighted images; T2, T2-weighted images; TOF, time-of-flight; JV, jugular vein.

the left common carotid artery (4 mm proximal (caudal) to the carotid bifurcation) using Vessel MASS software (Leiden University Medical Center, Leiden, the Netherlands) (13).

Morphological measurements were performed by one observer for each individual sequence (T1- and T2 sequence for lumen area and vessel wall area; TOF sequence for lumen area) for 3T and 7T images (Figure 2). To test intra-observer reproducibility, each scan was analyzed twice by one experienced observer (Observer 1, two years of experience in cardiac MRI). To test inter-observer reproducibility, the scans were analyzed by a second observer (Observer 2, one year experience of cardiac MRI) and data were compared with the first observer.

Measurements of image quality (SNR vessel wall (SNR_{VW}) and CNR lumen/wall) were performed by one observer (Observer 1) for the T1- and T2 sequences. In addition, the SNR_{VW} and CNR were compared between 3T and 7T taking into account the non-gaussian distribution of the signal close to zero (4). SNR was calculated as SNR= S/σ (14). S is the true signal intensity corrected for the noise contribution and is obtained by the measured signal (S_m) and the measured background signal (S_n): $S = (S_m^2 - S_n^2)^{1/2}$. The true standard deviation of the noise (σ) depends on the number of receivers. For 7T, when a single single receiver is used the measured standard deviation needs to be divided by 0.655 (11) to obtain σ. Although at 3T two receiver coils were used, the elements are spaced sufficiently apart (left and right side of the neck) such that coupling between the two is negligible. An identical correction factor was therefore applied to the data acquired at 3T and 7T.

CNR was calculated as the difference between vessel wall and lumen SNR: CNR= SNR vessel – SNR lumen. Signal intensity from the background noise was sampled by a manually drawn region of interest in the corner of each image, devoid of signal and artifact. Mean signal intensity ± standard deviation of the vessel wall area and lumen area were provided by the Vessel MASS software.

Statistical analysis

The correlation between morphologic measurements obtained at 3T and 7T MRI was tested with intraclass correlation (ICC) for absolute agreement. ICCs close to 1.0 indicate good agreement between two measurements. The mean differences between repeated measurements against the mean value of repeated scans were described by Bland-Altman plots (15). For the morphological measurements, both intra-observer and inter-observer mean relative errors (MREs) were calculated. For this calculation, the absolute difference between two measurements was calculated per volunteer and divided by the first measurement, to yield the relative error. Consecutively, the mean relative error (MRE) was then calculated.

SNR_{VW} and CNR values are expressed as median (interquartile range). Data from the different measurements were compared using the Wilcoxon signed ranks test for non-parametric paired observations. A p-value < 0.05 was considered statistically significant.

All statistical analyses were performed using SPSS v. 18.0 (SPSS, Chicago, IL).

RESULTS

All 18 volunteers underwent successful MRI scanning at the 3T and 7T MR system.

Lumen and vessel wall.

Figure 2 illustrates example carotid artery imaging of the left common carotid artery from a healthy volunteer at 3T and 7T.

The agreement between 3T and 7T images was calculated using the ICCs. An overview of the calculated ICCs and MRE (%) for the lumen area and vessel wall area is provided in Table 2. Morphologic carotid vessel wall measurements were comparable between 7T and 3T for both T1-weighted images (lumen area; ICC: 0.81, vessel wall area; ICC: 0.84), T2-weighted images (lumen area; ICC: 0.97, vessel wall area; ICC: 0.92) and TOF images (lumen area; ICC: 0.97).

Table 2. Results of Comparison of Morphological Measurements at Matched Location Between 3T and 7T

	3 T	7 T	3T vs 7T	
	Mean (SD) (mm^2)	Mean (SD) (mm^2)	MRE (%)	ICC (CI)
T1 Lumen area	33.16 (6.5)	31.07 (5.88)	5.8	0.85 (0.65; 0.94)
T1 Vessel wall area	17.83 (3.32)	17.17 (3.71)	3.8	0.85 (0.64; 0.94)
T2 Lumen area	33.11 (10.15)	33.28 (8.98)	1.8	0.97 (0.91; 0.99)
T2 Vessel wall area	16.36 (4.58)	16.62 (4.1)	2.8	0.91 (0.78; 0.97)
TOF Lumen area	34.91 (8.39)	34.54 (9.42)	1.5	0.97 (0.91; 0.99)

Abbreviations: 3T, 3 Tesla magnetic field strength; 7T, 7 Tesla magnetic field strength; T1, T1-weighted images; T2, T2-weighted images; TOF, time-of-flight; MRE, mean relative error; ICC; intraclass correlation coefficient.

The mean differences, for lumen and vessel wall area between 3T and 7T measurements are presented (Bland Altman plots) in Figure 3 for both the T1- and T2-weighted images and TOF images. No dependence of the difference vs. the mean was observed.

Furthermore, both intra-observer and inter-observer reproducibility (including ICCs and MRE) for lumen- and vessel wall measurements for both the 3T and the 7T acquisitions was calculated (Table 3). No trend for differences was observed for the intra- and inter-observer reproducibility between the field strengths.

SNR and CNR

Measurements of SNR_{VW} and CNR of the left carotid artery at 3T and 7T are presented in Figure 4. At 7T carotid vessel wall imaging provided a significant increase in SNR_{VW} and CNR for both the T1- ($p<0.001$) and T2-weighted images ($p<0.05$). The median gain factor for 7T T1-weighted images was 3.6 for SNR_{VW} and 2.8 for CNR. For T2-weighted images the median gain factor was 1.4 for SNR_{VW} and 1.3 for CNR. Examples (n=10) of T1-weighted images and T2-weighted images obtained at 7T are provided in Figure 5.

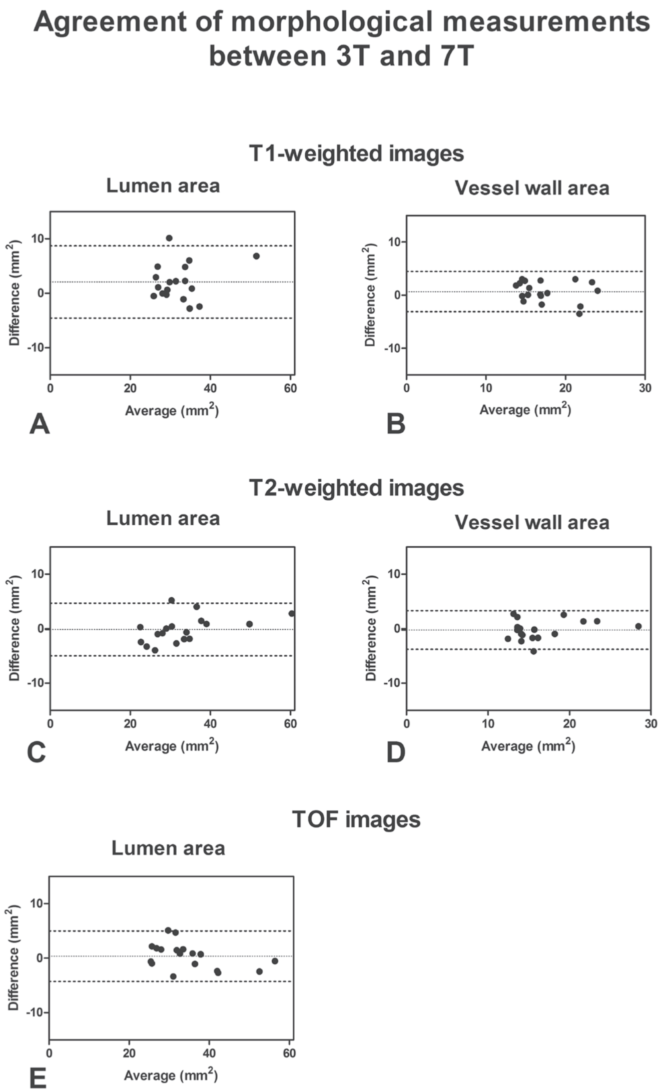

Figure 3. Agreement of morphological measurements between 3T and 7T. Bland-Altman plots for lumen area and vessel wall area, acquired at 3T and 7T, presented for T1-and T2-weighted images and TOF. **Figure 3A,B**: T1-weighted; **Figure C,D**: T2-weighted ; **Figure E**, TOF.
Abbreviations: 3T, 3 Tesla magnetic field strength; 7T, 7 Tesla magnetic field strength; T1, T1-weighted images; T2, T2-weighted images; TOF, time-of-flight.

Table 3. Intra-observer and Inter-observer Reproducibility of Morphologic Measurements

		Observer 1 Measurement 1	Observer 1 Measurement 2	Intra-observer		Observer 2	Inter-observer	
		Mean (SD) (mm²)	*Mean (SD)(mm²)*	*MRE %*	*ICC*	*Mean (SD) (mm²)*	*MRE %*	*ICC*
3T	**T1 Lumen area**	33.16 (6.5)	33.26 (6.8)	0.3	0.98 (0.95; 0.99)	33.76 (5.8)	2.6	0.89 (0.73; 0.96)
	T1 Vessel wall area	17.83 (3.32)	16.68 (1.6)	6	0.76 (0.43; 0.91)	16.86 (2.85)	4.7	0.77 (0.47; 0.91)
	T2 Lumen area	33.11(10.15)	33.27 (9.46)	1.1	0.99 (0.96; 0.99)	33.05 (8.11)	1.4	0.93 (0.83; 0.97)
	T2 Vessel wall area	16.36 (4.58)	16.23 (4.37)	0.14	0.93 (0.82; 0.97)	15.75 (3.2)	1.4	0.76 (0.47; 0.90)
	TOF Lumen area	34.91 (8.39)	34.22 (8.45)	1.8	0.96 (0.90; 0.99)	32.59 (8.65)	6.8	0.93 (0.55; 0.98)
7T	**T1 Lumen area**	31.07 (5.88)	30.35 (5.7)	2.2	0.96 (0.89; 0.99)	30.47 (6.6)	2.1	0.92 (0.79; 0.97)
	T1 Vessel wall area	17.17 (3.71)	17.4 (4.14)	1.5	0.90 (0.75; 0.96)	15.82 (3.09)	6.4	0.66 (0.28; 0.86)
	T2 Lumen area	33.28 (8.98)	34 (9.7)	2.0	0.98 (0.96; 0.99)	34.37 (9.8)	3.3	0.95 (0.88; 0.98)
	T2 Vessel wall area	16.62 (4.1)	16.4 (4.1)	1.1	0.96 (0.90; 0.99)	15.2 (3.33)	7.5	0.80 (0.42; 0.93)
	TOF Lumen area	34.54 (9.42)	34.93 (9.88)	1.1	0.99 (0.96; 1.00)	32.19 (8.73)	6.4	0.92 (0.64; 0.98)

Abbreviations: 3T, 3 Tesla magnetic field strength; 7T, 7 Tesla magnetic field strength; T1, T1-weighted images; T2, T2-weighted images; TOF, time-of-flight; MRE, mean relative error; ICC; intraclass correlation coefficient.

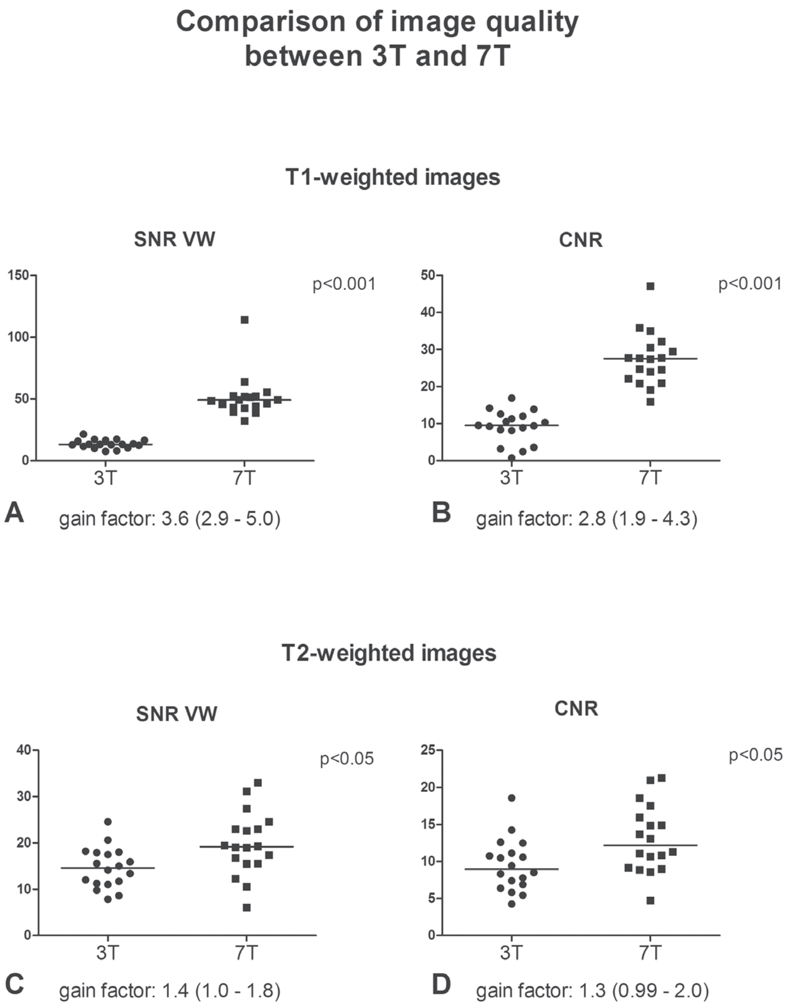

Figure 4. Comparison of image quality between 3T and 7T. Individual measurements are provided of signal-to-noise ratio of the carotid vessel wall (SNR_{VW}) and contrast to noise ratio (CNR) for T1-weighted and T2-weighted images 3T and 7T. **Figure A,B:** T1-weighted; **Figure C,D**: T2-weighted. Individual median gain factor (interquartile range) is provided.

Abbreviations: SNR_{VW} signal-to-noise-ratio for vessel wall; CNR, contrast-to-noise-ratio; 3T, 3 Tesla magnetic field strength; 7T, 7 Tesla magnetic field strength.

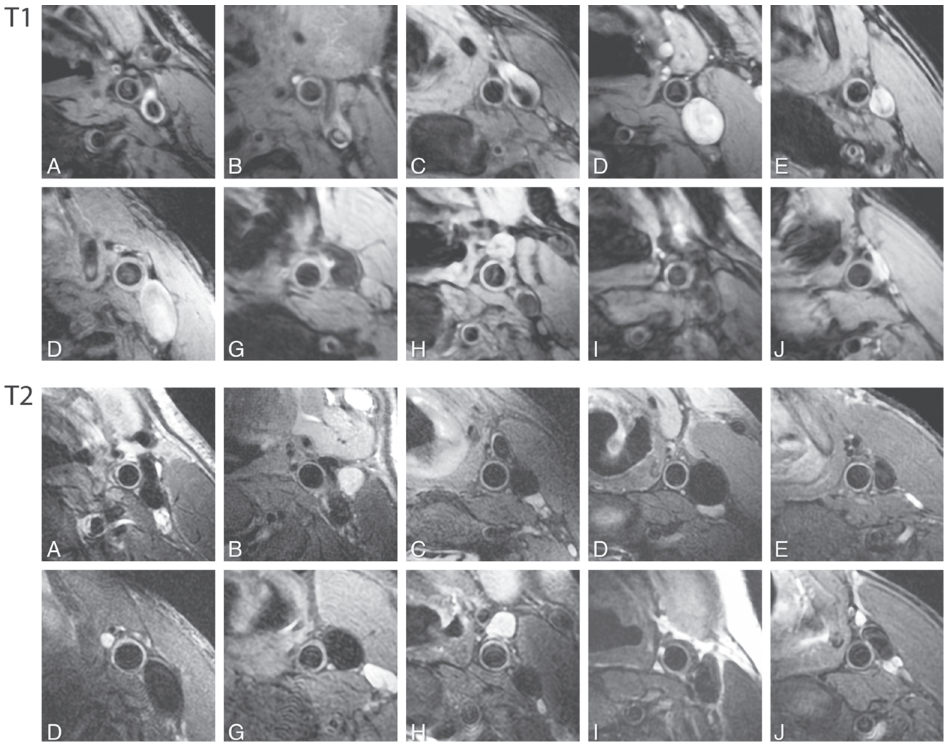

Figure 5. Examples of T1-weighted images and T2-weighted images obtained at 7T. From top to bottom: 10 examples of T1-weighted images (**A to J**) and the corresponding T2-weighted images (**A to J**). *Abbreviations:* T1, T1-weighted images; T2, T2-weighted images.

DISCUSSION

The present study, directly compares 3T and 7T carotid vessel wall imaging in healthy volunteers and demonstrates that in vivo carotid vessel wall imaging, with multi contrast protocol is technically feasible at ultra high-field 7T MR equipped with a custom-built RF transmit and receive surface coil. Furthermore, this is the first study comparing morphological measurements and measurements of image quality in a quantitative setting. The main findings of the study are: i) 7T BB common carotid vessel wall imaging, at a predefined position in the common carotid artery relative to the flow divider, is feasible using local saturation slabs, ii) morphologic carotid vessel wall measurements (lumen area and vessel wall area) and intra- and inter-observer reproducibility are comparable between 3T and 7T, iii) ultra high field 7T MRI carotid vessel wall imaging improves SNR_{VW} and CNR compared to 3T.

Our study highlights the potential of 7T carotid MR imaging for assessment of carotid lumen area and vessel wall area, since accurate delineation of the carotid artery vessel wall structure is crucial to detect carotid atherosclerosis and atherosclerotic changes of the vessel wall over time.

A recent study showed initial in vivo results of imaging of the carotid arteries at 7T in three volunteers (10). Estimation of luminal narrowing was performed with high-resolution MRA images, with a non-contrast 3D FLASH sequence. In addition, proton density(PD)/ T2 weighted turbo spin echo images were used for analysis of the carotid vessel wall (10).

The feasibility of carotid vessel wall imaging at 7T is further confirmed by the present study in a larger population and our data show that the feasibility of analysis of the vessel wall also extends to T1-weighted images obtained at 7T.

The present study also provided a comparison of the morphologic measurements at 3T versus 7T. In comparison with previous studies on vessel morphology, the agreement on interscan- and inter-observer reproducibility is in the same magnitude as observed at 3T (11,16).

Carotid vessel wall MRI at 7T is of significant interest because it may provide higher SNR_{VW} and CNR(3). As a consequence spatial resolution can be improved (8). These advances hold potential for more detailed assessment of carotid atherosclerotic plaque morphology (17). The present study provides a direct quantitative comparison for SNR_{VW} and CNR at 3T and 7T. SNR_{VW} and CNR values at 3T were in the same magnitude as previously shown by Underhill et al, comparing carotid vessel wall imaging at 1.5T and 3T (18). At ultra high field strength (7T), improved SNR_{VW} and CNR was observed in our study, both for the T1-weighted gradient echo ($p<0.001$) and for the T2-weighted turbo spin echo images ($P<0.005$). T1-weighted images are the cornerstone for identification of carotid plaque composition and therefore, the significant gains in image quality with median gain factors of 3.6 and 2.8 for SNR_{VW} and CNR respectively, may increase applications to improved carotid vessel wall imaging at ultra high field strength (19,20).

The improved SNR_{VW} and CNR suggest that 7T MRI is a potential technique to assess carotid atherosclerosis in more detail. The vessel wall area is thought to be a surrogate marker for atherosclerotic disease and detailed assessment of carotid atherosclerosis and plaque morphology permits assessment of disease burden (21-23) and identification of vulnerable patients who are at risk of future vascular events (22). A more detailed assessment of atherosclerosis may also permit an increased identification of changes in the carotid artery vessel wall structure over time and can be used to monitor progression of the disease or to monitor intervention (2).

The following limitations need to be acknowledged. Our study focused on the technical feasibility of 7T carotid vessel wall imaging of the common carotid artery in a population of healthy volunteers, without occlusive plaques or reduced flow. Whether carotid vessel wall imaging at 7T MR systems will lead to a better identification of atherosclerosis can not be concluded from the present study and therefore further study is warranted. In addition, 7T imaging of the internal and external carotid artery distal to the carotid bifurcation was not performed. Therefore the results of the present study (including the observed improvement in image quality at 7T) only relate to one slice of the common carotid artery. Further evaluation of the feasibility of carotid vessel wall imaging should involve; more challenging populations, i.e. patients with extensive carotid plaques, a longer trajectory of the carotid artery, bilateral carotid artery imaging and the development of dedicated coils at 7T. Indeed, carotid imaging is expected to benefit (in terms of penetration depth and image quality) from using more sophisticated transmit array coils as is shown in other applications at high field as well (3,6,10). Kraff et al. showed that when using a multi-element T/R coil at 7T it is possible to image both carotid arteries at the same time; however there are still image inhomogeneities present (10). In the current study, even though the coverage of the local T/R coil was limited, sufficient RF penetration was obtained for adequate visualization of one of the carotid arteries. The RF field was sufficiently homogeneous that with the proper sequence and hardware modification it was possible to achieve the most relevant image contrasts for carotid artery imaging (BB-T1, BB-T2 and TOF). Furthermore, while the design of our 7T feasibility study involved a comparison of 3T and 7T acquisitions, under identical conditions, in the future, the parameters of 7T imaging sequences need to be optimized for time efficiency.

In conclusion, this study shows our initial experience and feasibility of ultra-high field 7T MR carotid vessel wall imaging. Morphologic carotid vessel wall measurements were comparable between 7T and 3T. 7T MRI of the common carotid artery showed improved SNR_{VW} and CNR as compared to 3T MRI. Therefore, ultra-high field 7T vessel wall MRI may permit a more detailed assessment of carotid atherosclerosis and plaque morphology.

REFERENCES

1. Lloyd-Jones D, Adams RJ, Brown TM et al. Heart disease and stroke statistics—2010 update: a report from the American Heart Association. Circulation 2010;121:e46-e215.
2. Corti R, Fuster V. Imaging of atherosclerosis: magnetic resonance imaging. Eur Heart J 2011;32:1709-1719.
3. Niendorf T, Sodickson DK, Krombach GA, Schulz-Menger J. Toward cardiovascular MRI at 7 T: clinical needs, technical solutions and research promises. Eur Radiol 2010;20:2806-2816.
4. Umutlu L, Kraff O, Orzada S et al. Dynamic contrast-enhanced renal MRI at 7 Tesla: preliminary results. Invest Radiol 2011;46:425-433.
5. van Elderen SG, Versluis MJ, Webb AG et al. Initial results on in vivo human coronary MR angiography at 7 T. Magn Reson Med 2009;62:1379-1384.
6. Vaughan JT, Snyder CJ, DelaBarre LJ et al. Whole-body imaging at 7T: preliminary results. Magn Reson Med 2009;61:244-248.
7. Korteweg MA, Veldhuis WB, Visser F et al. Feasibility of 7 Tesla breast magnetic resonance imaging determination of intrinsic sensitivity and high-resolution magnetic resonance imaging, diffusion-weighted imaging, and (1)H-magnetic resonance spectroscopy of breast cancer patients receiving neoadjuvant therapy. Invest Radiol 2011;46:370-376.
8. van Elderen SG, Versluis MJ, Westenberg JJ et al. Right coronary MR angiography at 7 T: a direct quantitative and qualitative comparison with 3 T in young healthy volunteers. Radiology 2010;257:254-259.
9. Vaughan JT, Garwood M, Collins CM et al. 7T vs. 4T: RF power, homogeneity, and signal-to-noise comparison in head images. Magn Reson Med 2001;46:24-30.
10. Kraff O, Bitz AK, Breyer T et al. A transmit/receive radiofrequency array for imaging the carotid arteries at 7 Tesla: coil design and first in vivo results. Invest Radiol 2011;46:246-254.
11. Alizadeh DR, Doornbos J, Tamsma JT et al. Assessment of the carotid artery by MRI at 3T: a study on reproducibility. J Magn Reson Imaging 2007;25:1035-1043.
12. Versluis MJ, Kan HE, van Buchem MA, Webb AG. Improved signal to noise in proton spectroscopy of the human calf muscle at 7 T using localized B1 calibration. Magn Reson Med 2010;63:207-211.
13. Adame IM, van der Geest RJ, Wasserman BA, Mohamed MA, Reiber JH, Lelieveldt BP. Automatic segmentation and plaque characterization in atherosclerotic carotid artery MR images. MAGMA 2004;16:227-234.
14. Yarnykh VL, Terashima M, Hayes CE et al. Multicontrast black-blood MRI of carotid arteries: comparison between 1.5 and 3 tesla magnetic field strengths. J Magn Reson Imaging 2006;23:691-698.
15. Bland JM, Altman DG. Statistical methods for assessing agreement between two methods of clinical measurement. Lancet 1986;1:307-310.
16. Li F, Yarnykh VL, Hatsukami TS et al. Scan-rescan reproducibility of carotid atherosclerotic plaque morphology and tissue composition measurements using multicontrast MRI at 3T. J Magn Reson Imaging 2010;31:168-176.
17. Cury RC, Houser SL, Furie KL et al. Vulnerable plaque detection by 3.0 tesla magnetic resonance imaging. Invest Radiol 2006;41:112-115.
18. Underhill HR, Yarnykh VL, Hatsukami TS et al. Carotid plaque morphology and composition: initial comparison between 1.5- and 3.0-T magnetic field strengths. Radiology 2008;248:550-560.
19. Zhao X, Underhill HR, Yuan C et al. Minimization of MR contrast weightings for the comprehensive evaluation of carotid atherosclerotic disease. Invest Radiol 2010;45:36-41.

20. Kwee RM, van Engelshoven JM, Mess WH et al. Reproducibility of fibrous cap status assessment of carotid artery plaques by contrast-enhanced MRI. Stroke 2009;40:3017-3021.
21. Zhao XQ, Yuan C, Hatsukami TS et al. Effects of prolonged intensive lipid-lowering therapy on the characteristics of carotid atherosclerotic plaques in vivo by MRI: a case-control study. Arterioscler Thromb Vasc Biol 2001;21:1623-1629.
22. Corti R, Fuster V, Fayad ZA et al. Lipid lowering by simvastatin induces regression of human atherosclerotic lesions: two years' follow-up by high-resolution noninvasive magnetic resonance imaging. Circulation 2002;106:2884-2887.
23. Corti R, Fuster V, Fayad ZA et al. Effects of aggressive versus conventional lipid-lowering therapy by simvastatin on human atherosclerotic lesions: a prospective, randomized, double-blind trial with high-resolution magnetic resonance imaging. J Am Coll Cardiol 2005;46:106-112.